Impact of route of particle engineering on dissolution performance of posaconazole

Tianyi Xiang [1 #], Zijian Wang [1 #], Marina Solomos [2], Stephanus Axnanda [3], Chienhung Chen [3], Margaret Figus [3], Luke Schenck [2,*] and Changquan Calvin Sun [1,*]

[#] These authors contributed to this work equally

[1] Pharmaceutical Materials Science and Engineering Laboratory, Department of Pharmaceutics, College of Pharmacy, University of Minnesota, Minneapolis, MN 55455, USA

[2] Oral Formulation Sciences, Merck & Co., Inc., Rahway, NJ 07065, USA

[3] Analytical Research & Development Merck & Co., Inc., Rahway, NJ 07065, USA

**Corresponding authors:*

Changquan Calvin Sun (sunx0053@umn.edu)
Luke Schenck (luke.schenck@merck.com)

Abstract

Even when they have similar particle size, micron sized drug crystals prepared via different process routes may still exhibit considerable variability in pharmaceutical properties, due to the anisotropy of molecular crystals. This study aims to evaluate the dissolution performance of micronized posaconazole obtained through both milling and precipitation, with and without polymer coating. To overcome the problem of pressure-induced amorphization of posaconazole, powder dissolution was performed instead of intrinsic dissolution, which requires compressing powder into pellets. However, direct powder dissolution was challenged by the poor dispersibility of micronized posaconazole powders because of their extremely poor wettability. To solve this problem, we pretreated powders by dispersing them in an aqueous solution with a surfactant. Despite posaconazole forming a hydrate after pretreatment, differences in measured powder dissolution rates are meaningful in predicting impact of routes of API engineering on biopharmaceutical performance since hydration of posaconazole also occurs *in vivo*. This case study presents a systematic approach in addressing challenges when characterizing dissolution performance of drug powders.

Keywords: Posaconazole, dissolution, agglomeration, stability, micronization

1. Introduction

Oral solid dosage forms dominate the pharmaceutical market due to their excellent stability, good patient compliance, low manufacturing cost, and large production volume (Sun, 2009). For poorly soluble active pharmaceutical ingredients (API), achieving a high bioavailability of oral solid dosage forms is a challenge. This challenge can be addressed by several API engineering techniques, such as using a more soluble solid form (Li et al., 2022), using solubilizing agents in the formulation (Lalge et al., 2022), and using micronized API powders (Perumalla and Sun, 2014). The latter approach improves bioavailability by enhancing dissolution rate of APIs due to increased total surface area of API (Shekunov et al., 2007) (Yao et al., 2023).

Among common processing techniques, the "top-down" milling approach entails producing micron-sized particles through physical impacts and collisions (Wang et al., 2022). In contrast, the "bottom-up" fast precipitation approach obtains micronized particles through fast phase separation of API from solution. Due to the anisotropy of molecular crystals (Chung and Buessem, 1967) (Modi et al., 2014), different processing routes can lead to API batches with different bulk properties, even when particle sizes are comparable and the solid form is the same, if different crystal surfaces are presented (Wang et al., 2022). Varied breakage planes during milling and solvent interactions during precipitation could lead to the presence of different functional groups on crystal surfaces (Heng et al., 2006) (Bade et al., 2024). Meanwhile, fine particles (<10 microns) of a hydrophobic API can form agglomerates both in a dry powder and in aqueous media (Kendall, 1994), which can negate the potential dissolution advantages of micronized API. To overcome the problems of poor wettability (Gui et al., 2019) and weak bonding during tableting (Shi and Sun, 2010), particle coating has been employed. This versatile particle engineering technique can be accomplished through multiple routes, such as surface-controlled polymer precipitation (Wang et al., 2002) (Tirkkonen et al., 1994) (Lu et al., 2007), fluidized bed coating (Teunou and Poncelet, 2002) (Osei-Yeboah and Sun, 2015), and atomic layer deposition (Gui et al., 2019) (Li et al., 2019), spray-drying (Shi and Sun, 2011), mechanical dry coating (Yang et al., 2005) (Zhou et al., 2012). Here, the coating was applied during isolation, where material dissolved in the mother liquors is deposited on surfaces during drying (Coelho et al., 2022) (Hiew et al., 2023). It is also of practical importance to understand how API particle coating affects dissolution.

Posaconazole, an antifungal agent, is a fluorine-containing triazole molecule that has been marketed as amorphous solid dispersion-based tablets (Huang et al., 2019). We chose

posaconazole as a model compound to study the influence of processing routes on dissolution behaviors since *in vivo* data showed different bioavailability for batches delivered as an oral suspension of micronized API. The observation of slight changes in API properties resulting in *in vivo* exposure that was not bio-equivalent is similar to that reported in a previous publication (Wang et al., 2022). A likely reason for such variability in bioavailability is different dissolution behaviors of API batches. Hence, we sought to identify *in vitro* characterization that would have been predictive of the *in vivo* results. This involved systematically investigating the dissolution behavior of posaconazole batches prepared using different processing routes. This proved to be challenging using conventional techniques due to: 1) pressure-induced amorphization of posaconazole (Huang et al., 2019), which prevented the application of the intrinsic dissolution method using a rotating disc; 2) agglomeration of API particles due to poor wettability; and 3) hydration during the course of dissolution.

2. Materials and methods

2.1. Materials

Various lots of posaconazole were obtained from Merck & Co., Inc. (Rahway, NJ, USA). Sodium lauryl sulfate was purchased from Ward's Science (Rochester, NY). Poloxamer (Pluronic F127, Sigma-Aldrich, Milwaukee, WI, USA) was used as received. Hydrochloric acid (36.5%-38%; VWR International, Eagan, MN), acetone, sodium phosphate monobasic monohydrate, and sodium phosphate dibasic heptahydrate (Fisher Scientific International, Inc., Fair Lawn, NJ) were used as received to prepare buffer solutions.

2.2. Methods

2.2.1. Preparation of Samples

Lots M019 and M015 were obtained from production scale jet milling. Lot B1-1 was generated through a high shear direct precipitation (HSDP) process using the same solvent system employed in the crystallization of the parent, un-milled material used to generate M019 and M015. The HSDP utilized 40 g/L of posaconazole heated in acetone to dissolve. This was held at 50 ˚C and added to cooled de-ionized water (DIW). The DIW was recirculated through a jacketed vessel to maintain the batch temperature below 30 ˚C after addition, using the natural draw of a high shear rotor-stator mill (Quadro HV0 homogenizer, Quadro Engineering Corp., Waterloo, ON,

Canada), running at 70 m/s with the emulsion, which was approximately 18 L/min. The API in acetone was added at approximately 1.8 L/min (Harter et al., 2013). The final mother liquor composition was 2:1 water: acetone (13.3 g/L API concentration). The material was displacement washed with water, wherein water was used to rinse off residual acetone in the wet cake. This process ensures minimized the risk of particle agglomeration by taking advantage of the extremely low solubility of the API in water. After washing, the material was vacuum dried at 40˚C to remove all residual solvent.

Coating of the API crystals relied on material dissolved in capillary bound water in the wet cake post batch filtration. Following vacuum drying, solids dissolved in the water would be deposited onto the surfaces of the crystals. Here, previously dried API was re-suspended at 100 g/L and Poloxamer was suspended at 28 g/L in DI water, then homogenized with an IKA T25 Ultra-Turrax homogenizer (IKA Works, Inc., Wilmington, NC) mill at approximately 15 m/s to fully disperse any API aggregates but not break primary particles (Schenck et al., 2021). The batch was filtered on a medium-fit funnel. The loss-on-drying (LOD) at this point was approximately 52 wt%. The poloxamer was not expected to solubilize the posaconazole because its concentration (28 g/L) was significantly lower than the critical micelle concentration (50 g/L). Hence, physical losses of the API were minimal due to the low solubility of posaconazole (Yao et al., 2022). The approximate loading of poloxamer on the final dried API was determined to be approximately 3.0% in the case of lots M015 and M019 and 3.9% for batch 1-1. This could be calculated from the initial API quantity added, the poloxamer concentration in the mother liquors, the initial moisture content of the filtered wet cake before drying, and the final mass of the dried coated solids.

2.2.2. Particle Size Distribution

Particle size distribution (PSD) measurements were made using a laser (λ = 780 nm) diffraction particle size analyzer (Microtrac S3500, York, PA, USA), with scattered light ranging from 0.02° to 45° angle. The instrument was set for measuring irregular solid API particles, using a refractive index of 1.51. The circulating media was Isopar-G with refractive index of 1.42. particle size data was reported in volume distribution of particles . For each measurement, the sample was sonicated at 30 W for 120 s to disperse particle aggregates.

2.2.3. Powder X-ray Diffraction

Powder X-ray diffractograms (PXRD) were obtained using a powder X-ray diffractometer (PANalytical X'pert Pro, Westborough, MA, USA), using Cu Kα radiation (1.54056 Å). Samples were scanned with a step size of 0.02° and 1 s dwell time from 5° to 35° 2θ. The tube voltage and amperage were 45 kV and 40 mA, respectively.

2.2.4. Surface Area Analysis

The specific surface area of each API lot was obtained from analyzing nitrogen adsorption-isotherms at 77 K collected using a TriStar II analyzer (Micromeritics Instrument Corp., Norcross, GA, USA). Each material was loaded into a sample tube and degassed under nitrogen purge at 35 °C for 1 h before analysis. After cooling to room temperature, the tube was weighed and placed into the adsorption port of the instrument. A static adsorption mode was used including full equilibration after each adsorbate load, where a sufficient time was allowed for the pressure to stabilize and attain equilibrium. This process ensures the accuracy of measured adsorption volume, which is critical for calculating accurate surface area. The adsorption isotherms were measured over a relative pressure, p/p_0, range of 0.001–0.995. The surface area was calculated via the Brunauer–Emmett–Teller (BET) method using data in the relative pressure range from 0.10 to 0.30 (Brunauer et al., 1938).

2.2.5. Intrinsic Dissolution Rate by Rotating Disc Method

Intrinsic dissolution rate (IDR) was measured using a rotating disc method (Yao et al., 2024). Each powder was compressed at pressures of both 200 MPa and 400 MPa by a Universal Material Testing Machine (model 1485; Zwick/Roell, Ulm, Germany) with a custom-made stainless-steel die, against a flat stainless-steel disc for 2 min to prepare a pellet (6.39 mm in diameter). Compacts made at a lower compaction pressure had particles shedding during the IDR experiment, which resulted in an uncontrolled increase in surface area for dissolution, leading to under estimated IDR values.

The obtained pellets had a visually smooth surface that was coplanar with the surface of the die. While rotating at 300 rpm, the die was immersed in 300 mL pure ethanol in a water-jacketed beaker, controlled at 37 °C. A UV-vis fiber optic probe (Ocean Optics, Dunedin, FL, USA) was used to continuously monitor the UV absorbance of the solution at 257 nm corresponding to the absorbance peak. Absorbance was converted to a concentration-time profile based on a

previously constructed concentration–absorbance standard curve (Figure S1). The initial linear part of the dissolution curve was used for calculating the dissolution rate (Figure S2). Ethanol was used because reliable IDR values could not be obtained in aqueous media due to the low solubility of posaconazole.

2.2.6. Intrinsic Dissolution Rate by Powder Dissolution

A total of 1.0 mL of fully dispersed pretreated suspensions was pipetted into 300 mL dissolution medium (0.7 mM SDS with pH adjusted to 3) at 37 ˚C and stirred by an overhead stirring paddle at 100 rpm. Temperature was controlled using a circulating water bath. The concentration in the medium was monitored *in situ* by a UV–Vis fiber optic dip probe (Ocean Optics, Dunedin, FL) and converted to a concentration-time profile.

To overcome the problem of poor dispersibility of micronized posaconazole in water, due to its poor wettability, and to ensure complete dispersion of particles during powder dissolution, ~60 mg of sample was dispersed in 20 mL SDS solution in water (6 mM) in a glass vial under stirring by a magnetic stirring bar at 100 rpm. To determine an optimum pretreatment method, pretreated suspension (1 mL) after 0 min, 15 min, 60 min, 24 h, and 72 h was pipetted to the medium for measuring dissolution rate. Because the solubility of posaconazole in this medium is negligible (0.20 µg/mL) (Mudie et al., 2020), no change in dissolution profile is expected once a powder has been fully dispersed. Still, the medium was saturated by posaconazole, through dispersing powders of posaconazole in SDS aqueous solutions overnight and passed through a 0.45 µm membrane, to eliminate the possibility of any dissolution of posaconazole before the powder dissolution experiment. Pretreated samples at different time points were examined under a polarized light microscope (PLM) (Nikon Eclipse E200, Nikon, Tokyo, Japan). Digital images were captured using a DS-Fi1 microscope camera and analyzed to qualitatively assess dispersibility.

2.2.7. Statistical Analysis

To assess the statistical significance of difference, one-way analysis of variance (ANOVA) and Tukey's multiple comparisons test were performed using R Studio software (version 1.4.1564, Posit PBC, MA) for all API samples, at $p < 0.05$ level.

3. Results and Discussions

3.1 Solid form of samples

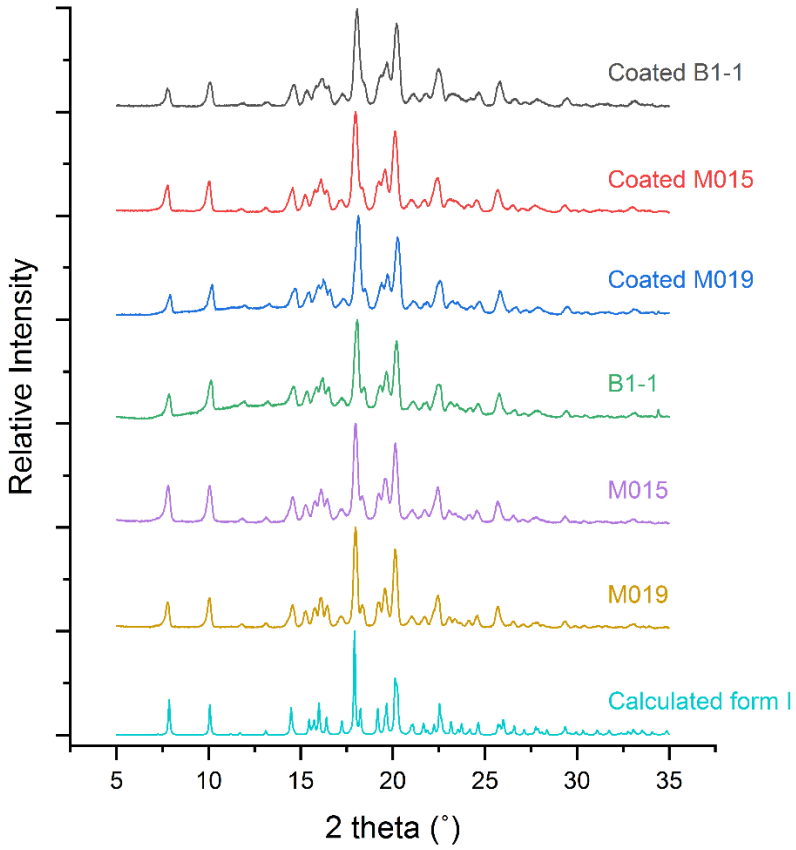

Figure 1. Powder X-ray diffraction patterns of coated and uncoated B1-1, M015, and M019, and the calculated pattern of Posaconazole form I.

The powder X-ray diffraction (PXRD) patterns of M019, M015, and B1-1 are substantially similar. They also matched the pattern calculated from the single crystal structure of posaconazole form I. Thus, these powders, despite being manufactured under different conditions, are all form I posaconazole. The PXRD patterns of the three coated samples also matched well with the PXRD patterns of corresponding uncoated powders. Thus, a qualitative comparison of the PXRD patterns suggests that the coating process did not induce any detectable changes in the solid form.

3.2 Agglomeration tendency

All posaconazole powders are highly cohesive, as expected for very fine powders. Visual inspection revealed the presence of large agglomerates of fine particles. Among the three uncoated

samples, B1-1 (prepared using precipitation method) showed the highest tendency for agglomeration, as indicated by a larger number of large chunks (Figure 2). Agglomerates in B1-1 are larger and harder to break compared to M015 and M019. The different agglomeration behavior of B1-1 cannot be attributed to larger surface area as its surface area is in between those of M019 and M015 (produced by jet milling), i.e., M015 > B1-1 > M019 (Table 1). It is likely that agglomerates formed in B1-1 during the filtration and drying, since there was no mechanical de-lumping step.

Figure 2. Photographs of different lots of posaconazole.

Table 1. Specific surface area and particle size distribution (PSD) of different batches of samples by BET measurement. Standard deviations are in parentheses.

Sample batch #	Specific surface area (m^2/g)	PSD (D50) (µm)
M019	2.8 (0.09)	5.0 (0.01)
M015	6.8 (0.05)	4.1 (0.01)
Batch 1-1	4.3 (0.03)	5.2 (0.01)

All coated samples have a lower agglomeration tendency than their corresponding uncoated samples, as indicated by the presence of fewer lumps (Figure 2). We attribute the lower agglomeration tendency of coated samples to the lower surface energy of the coating material, poloxamer, than posaconazole.

3.3. IDR by Rotating Disc Method

As an important solid-state property to distinguish varied solid forms (Yao et al., 2024) or different batches of the same API form (Wang et al., 2022), IDR is commonly measured by the rotating disc method, which is both material-sparing and convenient (Yu et al., 2004). However, the determination of IDR of posaconazole batches by the rotating disc method, which required compressing a powder into a pellet to generate a flat smooth surface with a defined exposed surface area, was hindered by its pressure-induced amorphization. It was estimated that ~23% of crystalline posaconazole would be amorphized after compaction at 400 MPa based on solid-state NMR results (Huang et al., 2019), which was also observed in this work when posaconazole was compressed under both 400 and 1000 MPa (Figure S3, Table S1 and S2). For this reason, IDR results of POS by this method were highly variable. For example, the IDR results of M019 measured by the rotating disc method in ethanol were both sensitive to pressure used to prepare a pellet and highly variable (Table 2). Due to the unreliability of the data, no conclusions or comparisons regarding the IDR between the two conditions can be made.

Table 2. Intrinsic dissolution rate (IDR) of M019 after compaction by the rotating disk method in ethanol (n = 5).

Pressure (MPa)	IDR ($\mu g \cdot cm^{-2} \cdot s^{-1}$)	RSD (%)
200	0.92 ± 0.26	28.3
400	0.56 ± 0.20	35.7

3.4. Dispersibility and Powder Dissolution

The stress sensitivity of posaconazole rendered IDR measurement by the rotating disc method inappropriate for comparing surface energetics among different batches since phase changes may be sample dependent. It was also expected that the majority of the phase change could be happening at the particle surfaces, with the resulting amorphous material confounding the assessment of the impact of preferred crystal orientation on dissolution behavior. Hence, we employed powder dissolution to measure IDR. In this approach, dissolution rate can be normalized by surface area of the sample to obtain IDR without needing to make a pellet with a known surface area (Tsinman et al., 2009). A prerequisite for obtaining an accurate IDR value by this method is to ensure complete dispersion of particles, i.e. absence of particle aggregation, in dissolution

medium. However, due to the high hydrophobicity, all batches of posaconazole underwent significant agglomeration during direct powder dissolution, regardless of whether or not they were coated (Figure 3). Therefore, the actual contact area between particles and dissolution medium is smaller than the surface area of the powder. In fact, no dissolution of posaconazole could be observed in 0.7 mM SDS aqueous solution at pH 3 at 37 °C. Despite the excellent aqueous solubility of poloxamers that should facilitate particle wetting, dissolution rates of all coated samples also remained nearly non-measurable, again due to limited surface area in contact with the medium.

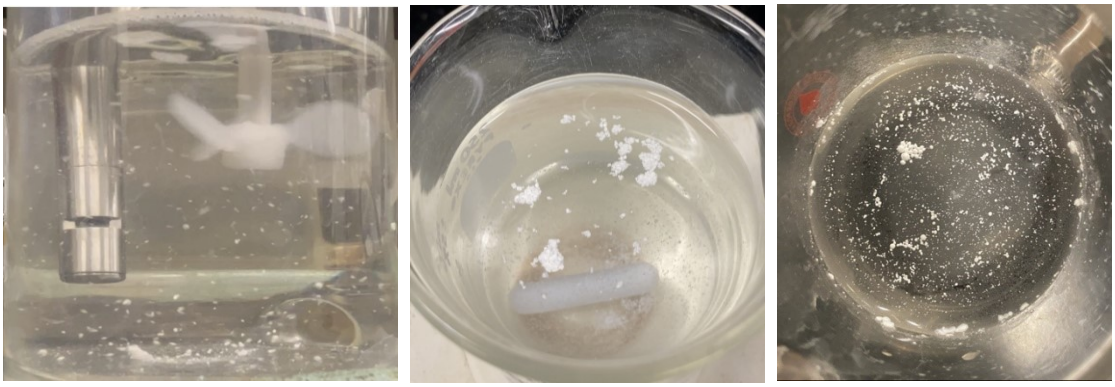

Figure 3. Poor wettability of micronized Posaconazole in a dissolution media of 0.7 mM SDS water solution at pH 3.

To resolve this issue, powders must be fully dispersed before dissolution testing. This was achieved in this work by pretreating powders in an SDS aqueous solution (1.73%, w/v, 6 mmol/L), saturated with posaconazole.

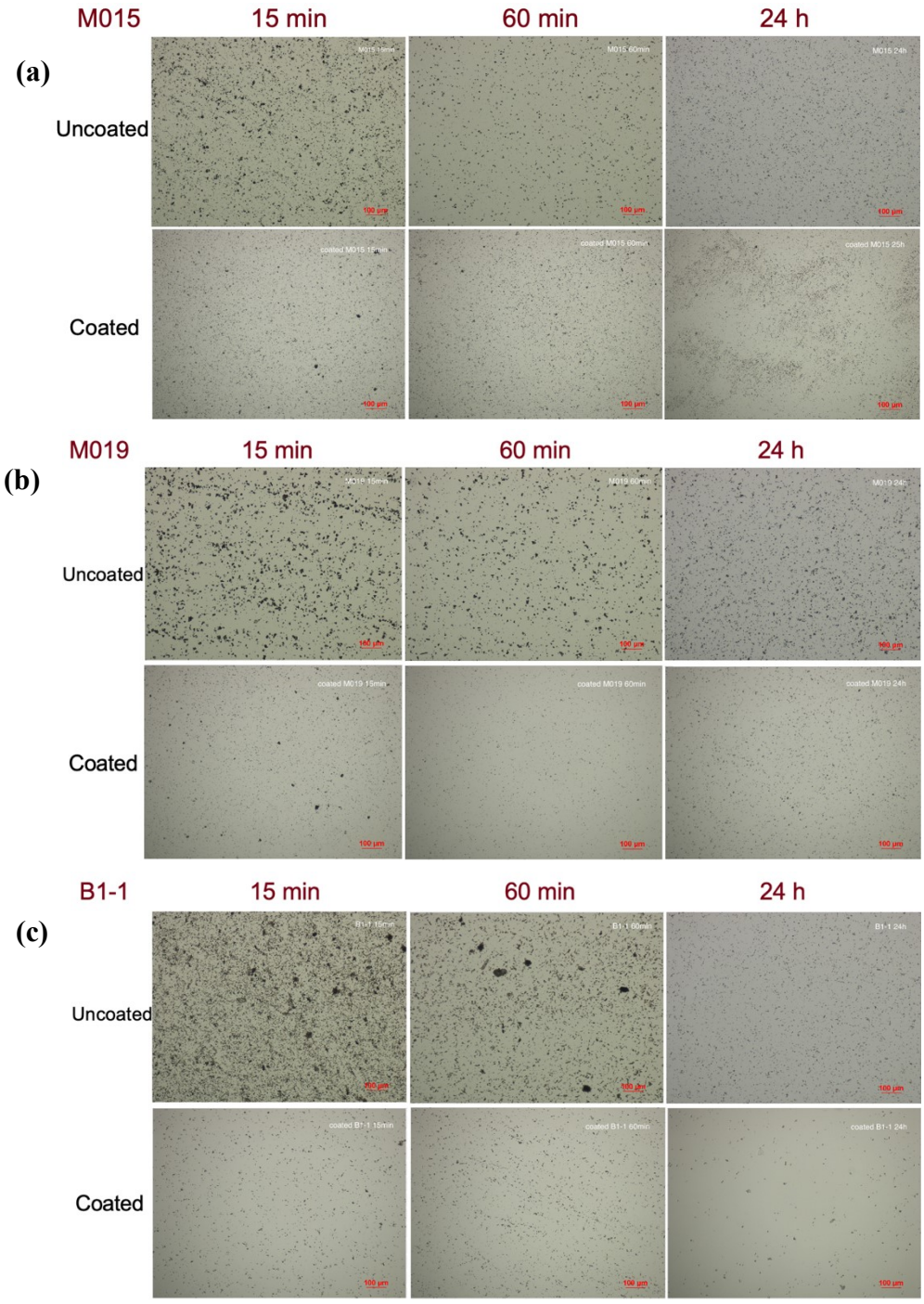

Figure 4. Polarized light microscopic images of suspended powders with different pretreatment times of a) M015; b) M019; and c) B1-1 of micronized posaconazole.

With increasing dispersion time of up to 24 hr during pretreatment, agglomerates disappeared completely in all samples. Samples coated by poloxamers could be more easily

dispersed than corresponding uncoated posaconazole powders. When observed under PLM, dispersions of coated samples had no visible agglomerates after 60 min pretreatment, but agglomerates could be seen in dispersion of uncoated samples (Figure 4). Effectiveness of pretreatment at different time points is also assessed from IDR measured. It is fair to conclude that 60 minutes is sufficient to achieve full dispersion for coated M015 and M019. However, this process requires up to 24 hours for uncoated M015 and M019. For B1-1, both coated and uncoated samples require 24 hours to complete dispersion during the pretreatment. This conclusion was also echoed by the dissolution rate data discussed below.

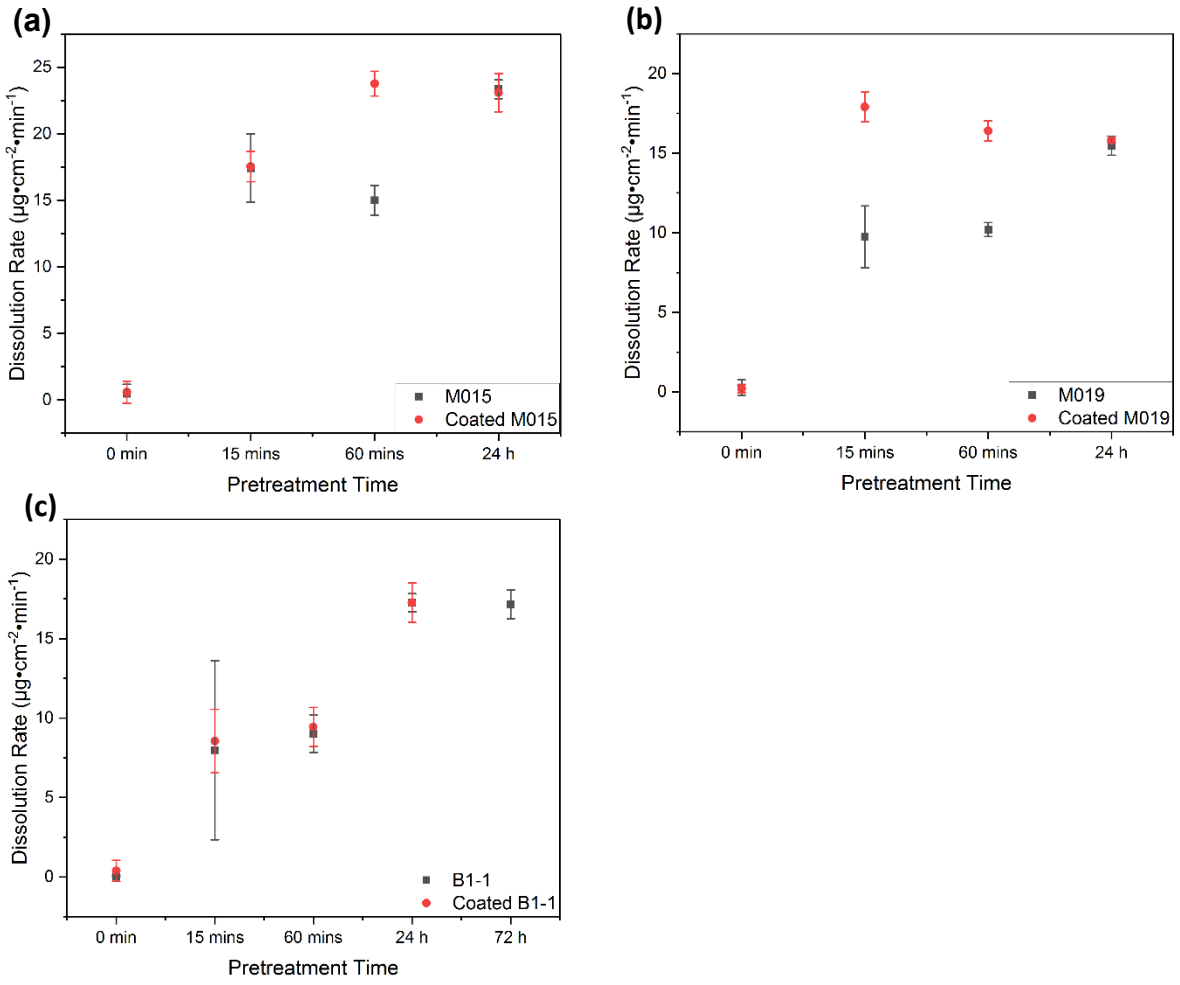

Figure 5. Dissolution rates of coated and uncoated posaconazole batches after different pretreatment times, a) M015; b) M019; c) B1-1.

An inspection of the IDR vs. pretreatment time profiles suggests that all powders were better dispersed over time, given the increase in IDR with time. For coated M015, the dissolution rate of the coated sample increases with increasing pretreatment time, but remains unchanged between 60 min and 24 hr (Figure 5a). This suggests complete dispersion of particles after 60 min. However, 60 min of pretreatment was not enough to completely disperse uncoated M015 batch since the IDR is significantly higher after 24 hr of pretreatment. The identical IDR of both coated and uncoated after 24 hr of pretreatment suggests that 1) both powders were fully dispersed after 24 hr of pretreatment and 2) coating did not change surface area of posaconazole. We note here that the small amount of poloxamer coating is expected to be fully dissolved in the pretreatment medium, exposing core posaconazole in subsequent powder dissolution process.

For M019, trends similar to M015 were observed (Figure 5b). The only difference is that the IDR of coated M019 reaches a plateau after 15 min of pretreatment, which is significantly shorter than that for coated M019 (60 min). Again, the identical IDR for the coated and uncoated samples after 24 hr of pretreatment confirms full dispersion and identical surface area between the two samples. For B1-1, poloxamer coating did not significantly affect dispersion effectiveness of pretreatment since the IDR – pretreatment time profiles are identical between the coated and uncoated samples (Figure 6c); both increased with time up to 24 hr. In order to confirm that complete dispersion was achieved at 24 hr, IDR of an uncoated B1-1 sample after 72 hr of pretreatment was also measured. The identical IDR values at 24 hr and 72 hr confirm no further change in surface area after 48 hr additional pretreatment, affirming complete dispersion after 24 hr.

3.5. Effects of Processing Route on Intrinsic Dissolution Rate

The apparent powder dissolution rates (ADR) of the three posaconazole batches are significantly different, following the descending order of M015 > B1-1 > M019 (Figure 6a). ADR was determined by taking the slopes of concentration-time powder dissolution profiles within the initial 20 s after suspensions were administrated (Figure S2). Their IDR values (after 24 hr of pretreatment) are also significantly different, following the descending order of M019 > B1-1 > M015 (Figure 6b). The different rank orders of the three API batches based on ADR and IDR were caused by the different specific surface areas (Table 1). Thus, both the different surface energetics

and surface area contribute to different biopharmaceutical performances among different batches of posaconazole.

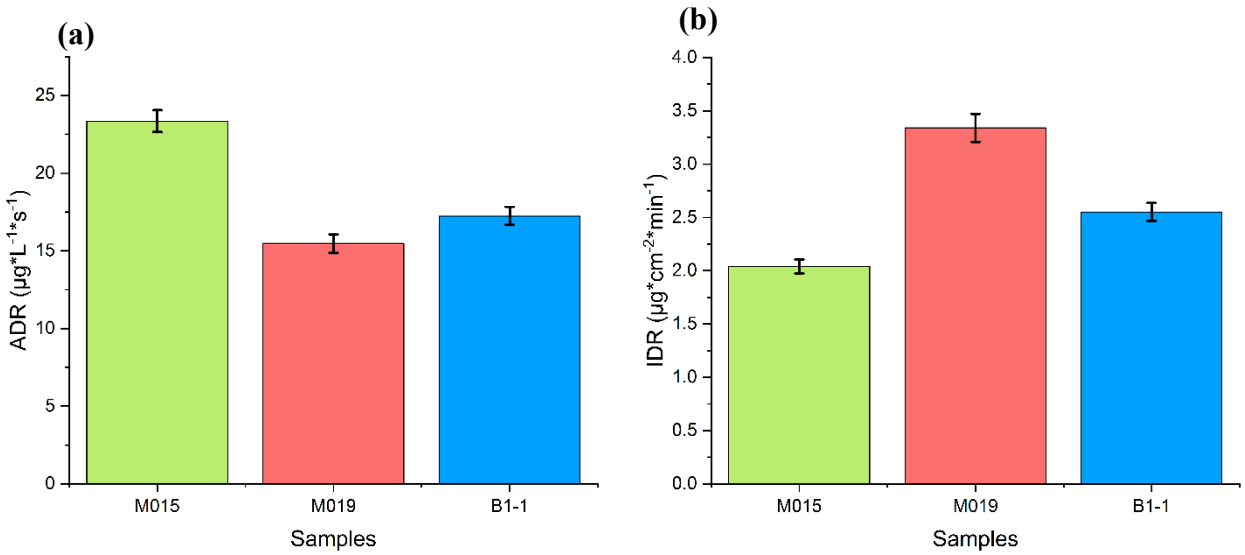

Figure 6. The powder dissolution rates of fully dispersed posaconazole batches, a) as measured; b) normalized by surface area.

3.6. Further complication by hydrate formation

As detailed in preceding sections, prolonged pretreatment is required in order to measure IDR of micron-sized posaconazole to understand process-induced differences in surface energetics of API. Such a pretreatment strategy should be valid for many other APIs. However, IDR values could also be affected by any phase conversion during pretreatment. For posaconazole, form I was observed to form a channel hydrate (form S) after sonicating an aqueous dispersion for 10 min (Lykouras et al., 2023) (Guidetti et al., 2024). This hydrate is thought to be isostructural to form I based on known crystallographic information of the two crystal forms (Table 3) (Lykouras et al., 2023), which means similar PXRD patterns. Fortunately, form S has characteristic peaks at around 10 ˚ and 25 ˚. We evaluated this potential phase conversion by examining uncoated M015 powder with PXRD after 15 min pretreatment (Figure 7), which confirmed the conversion into form S. Given the 24 hr of pretreatment required to attain full particle dispersion, it is likely that all powders had converted into form S in the powder dissolution study. Thus, the IDR values determined are those of the posaconazole hydrate of each starting material instead of form I.

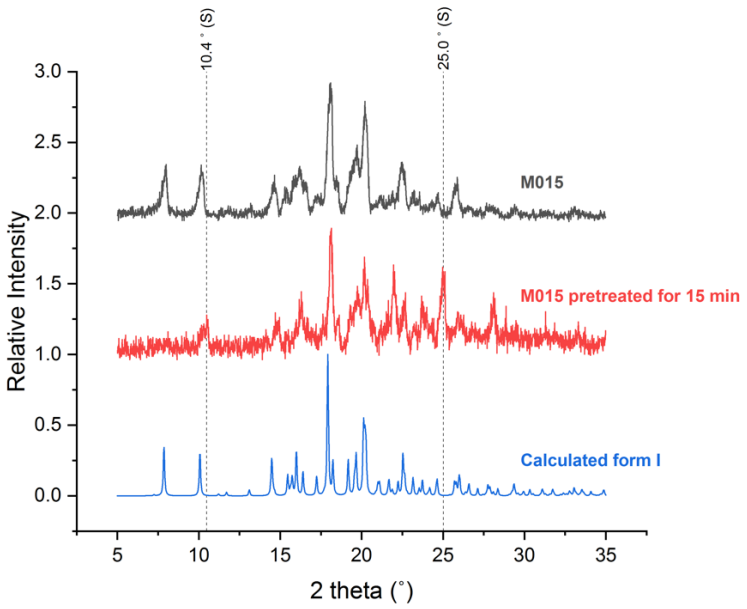

Figure 7. PXRD of M015, pretreated M015 for 15 min, and calculated posaconazole form I.

Table 3. Crystallographic parameters of Form I and Form S of posaconazole (regenerated from Lykouras et al., 2024) and (Lykouras et al., 2023).

Crystallographic Data	Form I	Form-S
Crystal System	Monoclinic	Monoclinic
Bravais Crystal Lattice	Simple Monoclinic	Simple Monoclinic
a **(Å)**	12.536 (0.001)	12.380 (0.005)
b **(Å)**	6.348 (0.0001)	6.305 (0.003)
c **(Å)**	22.780 (0.001)	23.126 (0.016)
β **(°)**	96.387 (0.002)	93.140 (0.034)
Unit Cell Volume (Å^3)	1801.48 (0.10)	1802.47 (1.68)

However, since the same phase conversion during powder dissolution would have also occurred *in vivo*, the IDR values measured in this work remain useful for understanding the impact of processing route on biopharmaceutical performance of posaconazole.

4. Conclusions

Variability in bioavailability for various lots of API meeting size specifications suggests the potential impact of crystal surface anisotropy on critical quality attributes, including dissolution and *in vivo* exposure. This work sought to identify *in vitro* characterization routes to discriminate

differences in properties of micronized API. This involved systematically studying the dissolution performance of micronized posaconazole produced by different processing routes, overcoming the challenges of 1) pressure-induced amorphization, and 2) agglomeration of particles during dissolution due to the poor wettability. The coating layer of poloxamer both improved the dispersibility and partially prevented the pressure-induced amorphization of jet milled samples but had no impact on precipitated samples. The IDR values, determined from the powder dissolution experiments, followed a descending order of M019 (jet milled) > B1-1 (precipitated) > M015 (jet milled). This, along with different surface areas of these batches, leads to apparent dissolution rates in the descending order of M015 > B1-1 > M019. Approaches taken in this work to measure the IDR for poorly water soluble posaconazole may benefit future dissolution characterization of other poorly soluble APIs.

Acknowledgements

C.C.S. thanks the National Science Foundation for support through the Industry University Collaborative Research Center grant IIP-2137264, Center for Integrated Materials Science and Engineering for Pharmaceutical Products (CIMSEPP).

Author Contributions

Conceptualization, L.S. and C.C.S.; Formal analysis, T.X., Z.W., C.C. and M.F.; Investigation, T.X., Z.W., M.S., S.A., C.C. and M.F.; Methodology, T.X., Z.W. and C.C.; Project administration, C.C.S., S.A. and L.S.; Resources, C.C.S., M.S., C.C. and M.F.; Writing—original draft, T.X.; Writing—review & editing, Z.W., M.S., S.A., L.S. and C.C.S. All authors have read and agreed to the published version of the manuscript.

References

Bade, I., Karde, V., Schenck, L., Solomos, M., Figus, M., Chen, C., Axnanda, S., Heng, J.Y.Y., 2024. Process-Induced Crystal Surface Anisotropy and the Impact on the Powder Properties of Odanacatib. Pharmaceutics 16. https://doi.org/10.3390/pharmaceutics16070883

Brunauer, S., Emmett, P.H., Teller, E., 1938. Adsorption of gases in multimolecular layers. J. Am. Chem. Soc. 60, 309–319.

Chung, D.H., Buessem, W.R., 1967. The Elastic Anisotropy of Crystals. J. Appl. Phys. 38, 2010–2012. https://doi.org/10.1063/1.1709819

Coelho, A., Schenck, L., Guner, G., Punia, A., Bilgili, E., 2022. A Combined Isolation and Formulation Approach to Convert Nanomilled Suspensions into High Drug-Loaded Composite Particles That Readily Reconstitute. Powders 1, 88–110. https://doi.org/10.3390/powders1020008

Gui, Y., Chen, Y., Chen, Z., Jones, K.J., Yu, L., 2019. Improving Stability and Dissolution of Amorphous Clofazimine by Polymer Nano-Coating. Pharm. Res. 36, 67. https://doi.org/10.1007/s11095-019-2584-9

Guidetti, M., Hilfiker, R., Kuentz, M., Bauer-Brandl, A., Blatter, F., 2024. Water-mediated phase transformations of posaconazole: An intricate jungle of crystal forms. Eur. J. Pharm. Sci. 195, 106722.

Harter, A., Schenck, L., Lee, I., Cote, A., 2013. High-Shear Rotor–Stator Wet Milling for Drug Substances: Expanding Capability with Improved Scalability. Org. Process Res. Dev. 17, 1335–1344. https://doi.org/10.1021/op4001143

Heng, J.Y.Y., Thielmann, F., Williams, D.R., 2006. The Effects of Milling on the Surface Properties of Form I Paracetamol Crystals. Pharm. Res. 23, 1918–1927. https://doi.org/10.1007/s11095-006-9042-1

Hiew, T.N., Saboo, S., Zemlyanov, D.Y., Punia, A., Wang, M., Smith, D., Lowinger, M., Solomos, M.A., Schenck, L., Taylor, L.S., 2023. Improving Dissolution Performance and Drug Loading of Amorphous Dispersions Through a Hierarchical Particle Approach. J. Pharm. Sci. 112, 2057–2068. https://doi.org/10.1016/j.xphs.2022.12.019

Huang, C., Klinzing, G., Procopio, A., Yang, F., Ren, J., Burlage, R., Zhu, L., Su, Y., 2019. Understanding Compression-Induced Amorphization of Crystalline Posaconazole. Mol. Pharm. 16, 825–833. https://doi.org/10.1021/acs.molpharmaceut.8b01122

Kendall, K., 1994. Adhesion: Molecules and Mechanics. Science 263, 1720–1725. https://doi.org/10.1126/science.263.5154.1720

Lalge, R., Kaur, N., Duggirala, N.K., Suryanarayanan, R., 2022. Dual Functionality of Bile Acid: Physical Stabilization of Drugs in the Amorphous Form and Solubility Enhancement in Solution. Mol. Pharm. 19, 2595–2606.

Li, J., Duggirala, N.K., Kumar, N.S.K., Su, Y., Suryanarayanan, R., 2022. Design of Ternary Amorphous Solid Dispersions for Enhanced Dissolution of Drug Combinations. Mol. Pharm. 19, 2950–2961. https://doi.org/10.1021/acs.molpharmaceut.2c00307

Li, Y., Yu, J., Hu, S., Chen, Z., Sacchetti, M., Sun, C.C., Yu, L., 2019. Polymer Nanocoating of Amorphous Drugs for Improving Stability, Dissolution, Powder Flow, and Tabletability: The Case of Chitosan-Coated Indomethacin. Mol. Pharm. 16, 1305–1311. https://doi.org/10.1021/acs.molpharmaceut.8b01237

Lu, B., Wen, R., Yang, H., He, Y., 2007. Sustained-release tablets of indomethacin-loaded microcapsules: Preparation, in vitro and in vivo characterization. Int. J. Pharm. 333, 87–94. https://doi.org/10.1016/j.ijpharm.2006.10.002

Lykouras, M., Orkoula, M., Kontoyannis, C., 2023. Formation and Characterisation of Posaconazole Hydrate Form. Pharmaceuticals 16. https://doi.org/10.3390/ph16010065

Modi, S.R., Dantuluri, A.K.R., Perumalla, S.R., Sun, C.C., Bansal, A.K., 2014. Effect of Crystal Habit on Intrinsic Dissolution Behavior of Celecoxib Due to Differential Wettability. Cryst. Growth Des. 14, 5283–5292. https://doi.org/10.1021/cg501084a

Mudie, D.M., Stewart, A.M., Biswas, N., Brodeur, T.J., Shepard, K.B., Smith, A., Morgen, M.M., Baumann, J.M., Vodak, D.T., 2020. Novel High-Drug-Loaded Amorphous

Dispersion Tablets of Posaconazole; In Vivo and In Vitro Assessment. Mol. Pharm. 17, 4463–4472. https://doi.org/10.1021/acs.molpharmaceut.0c00471
Osei-Yeboah, F., Sun, C.C., 2015. Tabletability Modulation Through Surface Engineering. J. Pharm. Sci. 104, 2645–2648. https://doi.org/10.1002/jps.24532
Perumalla, S.R., Sun, C.C., 2014. Enabling Tablet Product Development of 5-Fluorocytosine Through Integrated Crystal and Particle Engineering. J. Pharm. Sci. 103, 1126–1132. https://doi.org/10.1002/jps.23876
Schenck, L., Neri, C., Jia, X., Schafer, W., Axnanda, S., Canfield, N., Li, F., Shah, V., 2021. A Co-Processed API Approach for a Shear Sensitive Compound Affording Improved Chemical Stability and Streamlined Drug Product Processing. J. Pharm. Sci. 110, 3238–3245. https://doi.org/10.1016/j.xphs.2021.05.013
Shekunov, B.Y., Chattopadhyay, P., Tong, H.H.Y., Chow, A.H.L., 2007. Particle Size Analysis in Pharmaceutics: Principles, Methods and Applications. Pharm. Res. 24, 203–227. https://doi.org/10.1007/s11095-006-9146-7
Shi, L., Sun, C.C., 2011. Overcoming Poor Tabletability of Pharmaceutical Crystals by Surface Modification. Pharm. Res. 28, 3248–3255. https://doi.org/10.1007/s11095-011-0518-2
Shi, L., Sun, C.C., 2010. Transforming powder mechanical properties by core/shell structure: compressible sand. J. Pharm. Sci. 99, 4458–4462.
Sun, C.C., 2009. Materials Science Tetrahedron—A Useful Tool for Pharmaceutical Research and Development. J. Pharm. Sci. 98, 1671–1687. https://doi.org/10.1002/jps.21552
Teunou, E., Poncelet, D., 2002. Batch and continuous fluid bed coating – review and state of the art. J. Food Eng. 53, 325–340. https://doi.org/10.1016/S0260-8774(01)00173-X
Tirkkonen, S., Turakka, L., Paronen, P., 1994. Microencapsulation of indomethacin by gelatin-acacia complex coacervation in the presence of surfactants. J. Microencapsul. 11, 615–626. https://doi.org/10.3109/02652049409051111
Tsinman, K., Avdeef, A., Tsinman, O., Voloboy, D., 2009. Powder Dissolution Method for Estimating Rotating Disk Intrinsic Dissolution Rates of Low Solubility Drugs. Pharm. Res. 26, 2093–2100. https://doi.org/10.1007/s11095-009-9921-3
Wang, Y., Wei, D., Dave, R., Pfeffer, R., Sauceau, M., Letourneau, J.-J., Fages, J., 2002. Extraction and precipitation particle coating using supercritical CO2. Powder Technol. 127, 32–44. https://doi.org/10.1016/S0032-5910(02)00102-X
Wang, Z., Solomos, M., Axnanda, S., Chen, C., Figus, M., Schenck, L., Sun, C.C., 2022. Varied Bulk Powder Properties of Micro-Sized API within Size Specifications as a Result of Particle Engineering Methods. Pharmaceutics 14. https://doi.org/10.3390/pharmaceutics14091901
Yang, J., Sliva, A., Banerjee, A., Dave, R.N., Pfeffer, R., 2005. Dry particle coating for improving the flowability of cohesive powders. Prof Dr-Ing Otto Molerus 70th Birthd. 158, 21–33. https://doi.org/10.1016/j.powtec.2005.04.032
Yao, X., Borchardt, K.A., Gui, Y., Guzei, I.A., Zhang, G.G., Yu, L., 2022. Surface-enhanced crystal nucleation and polymorph selection in amorphous posaconazole. J. Chem. Phys. 157.
Yao, X., Xiang, T., Chen, S., Alagbe, B.D., Zhang, G.G.Z., Hong, R.S., Sun, C.C., Yu, L., Sheikh, A.Y., 2024. Efficient determination of critical water activity and classification of hydrate-anhydrate stability relationship. J. Pharm. Sci. https://doi.org/10.1016/j.xphs.2024.06.012

Yao, X., Yu, L., Zhang, G.G.Z., 2023. Impact of Crystal Nuclei on Dissolution of Amorphous Drugs. Mol. Pharm. 20, 1796–1805. https://doi.org/10.1021/acs.molpharmaceut.2c00989

Yu, L.X., Carlin, A.S., Amidon, G.L., Hussain, A.S., 2004. Feasibility studies of utilizing disk intrinsic dissolution rate to classify drugs. Int. J. Pharm. 270, 221–227. https://doi.org/10.1016/j.ijpharm.2003.10.016

Zhou, Q., Shi, L., Chattoraj, S., Sun, C.C., 2012. Preparation and Characterization of Surface-Engineered Coarse Microcrystalline Cellulose Through Dry Coating with Silica Nanoparticles. J. Pharm. Sci. 101, 4258–4266. https://doi.org/10.1002/jps.23301